European Journal of Pharmaceutical Sciences 198 (2024) 106791

Contents lists available at ScienceDirect

European Journal of Pharmaceutical Sciences

journal homepage: www.elsevier.com/locate/ejps

A study of hydrophobic domain formation of polymeric drug precipitation inhibitors in aqueous solution

Egis Zeneli [a,b], Justus Johann Lange [c], René Holm [d], Martin Kuentz [a,*]

[a] Institute of Pharma Technology, University of Applied Sciences and Arts Northwestern Switzerland, Hofackerstr. 30, Muttenz CH-4132, Switzerland
[b] Institute of Pharmaceutical Technology, University of Basel, Basel, Switzerland
[c] School of Pharmacy, University College Cork, Cork, Ireland
[d] Department of Physics, Chemistry and Pharmacy, University of Southern Denmark, Odense, Denmark

ARTICLE INFO

Keywords:
Solubility
Pharmaceutical polymers
Hydrophobic domains
Drug supersaturation
Drug precipitation inhibition

ABSTRACT

Despite the widespread use of polymers as precipitation inhibitors in supersaturating drug formulations, the current understanding of their mechanisms of action is still incomplete. Specifically, the role of hydrophobic drug interactions with polymers by considering possible supramolecular conformations in aqueous dispersion is an interesting topic. Accordingly, this study investigated the tendency of polymers to create hydrophobic domains, where lipophilic compounds may nest to support drug solubilisation and supersaturation. Fluorescence spectroscopy with the environment-sensitive probe pyrene was compared with atomistic molecular dynamics simulations of the model drug fenofibrate (FENO). Subsequently, kinetic drug supersaturation and thermodynamic solubility experiments were conducted. As a result, the different polymers showed hydrophobic domain formation to a varying degree and the molecular simulations supported interpretation of fluorescence spectroscopy data. Molecular insights were gained into the conformational structure of how the polymers interacted with FENO in solution phase, which apart from nucleation and crystal growth effects, determined drug concentrations in solution. Notable was that even at the lowest polymer concentration of 0.01 %, w/v, there were polymer-specific solubilisation effects of FENO observed and the resulting reduction in apparent drug supersaturation provided relevant knowledge both from a mechanistic and practical perspective.

1. Introduction

It is well known that poor water solubility poses a major obstacle to the industrial drug development pipeline. The number of poorly soluble compounds in drug discovery continuously increases, but even more concerning is that the extent of insolubility has worsened over the years (Taylor and Zhang, 2016). Thirty years ago an equilibrium solubility of 100 μg/mL would have been considered a concern, whereas today's scientists are often confronted with compounds having an equilibrium solubility in the nanogram range (Taylor and Zhang, 2016). Various formulation approaches have been used over the years to improve the apparent solubility of drug candidates, including the development of nanosuspensions, lipid-based formulations, and solid dispersions (Tres et al., 2018; Warren et al., 2010). For several compounds, dissolution enhancement alone may not be sufficient to cope with erratic drug absorption, hence an increase of the apparent drug solubility is often targeted (Boyd et al., 2019). In supersaturated drug delivery systems (SDDSs), the active ingredient is in a high energy form, which allows for intraluminal concentrations greater than the equilibrium solubility and hence a potential for better intestinal absorption (Boyd et al., 2019; Sharma and Jain, 2010). However, SDDSs and other supersaturatable formulations come with the challenge that unstable drug concentrations may not only drive permeation but have potential to cause luminal nucleation and growth (Chavan et al., 2016; Warren et al., 2010). The most frequently used approach to maintain drug supersaturation is the use of precipitation inhibitors such as surfactants, cyclodextrins, or polymers. Amidst these, the use of polymers is the most common choice (Boyd et al., 2019). These polymeric precipitation inhibitors (PPIs) can either interfere with drug precipitation by direct interactions in the solution phase or by adsorption of the polymer onto the surface of nuclei and crystals to inhibit their growth (Feng et al., 2018; Price et al., 2019). Polymers such as polyvinylpyrrolidone (PVP) or hydroxypropyl methylcellulose (HPMC) have demonstrated to efficiently maintain drug supersaturation (Chavan et al., 2016). However, it seems that

* Corresponding author.
E-mail address: martin.kuentz@fhnw.ch (M. Kuentz).

https://doi.org/10.1016/j.ejps.2024.106791
Received 9 November 2023; Received in revised form 17 April 2024; Accepted 3 May 2024
Available online 4 May 2024

supersaturation maintenance is greatly variable, depending on the studied drug (Chavan et al., 2016). Despite the widespread use of polymers as precipitation inhibitors, there are still mechanistic aspects that require further investigation. A general aspect of different mechanisms in the solution phase or on the surface of nuclei and crystals is that relevant drug-polymer interactions must be formed to obtain a suitable PPI (Aleandri et al., 2018). Understanding molecular interactions between drug and polymer is of great importance to clarify their precipitation inhibition capacity. Although this has been the subject of several studies, the three-dimensional conformations of PPIs in solution phase, which can form hydrophobic domains for drugs to interact, is an underexplored field of research. Moreover, pharmaceutical scientists have focused traditionally on ionic interactions or hydrogen bonding, but there is in recent years a growing awareness that hydrophobic drug interactions with PPIs can be highly relevant (Zhao et al., 2023). Though hydrophobic interactions are typically much weaker than electrostatic interactions or hydrogen bonding per contact point, the long-range Van der Waals forces may come in a high number of contacts leading to a considerable net interaction between molecules (Meyer et al., 2006). Hydrophobic interactions prove to be a challenging topic, due to the difficulty of providing unambiguous contribution of hydrophobicity to the overall molecular interactions (Ditzinger et al., 2019; Ducker and Mastropietro, 2016). An example is a study on the dissolution behavior of FENO from solid dispersions (SDs) in the presence of polyethylene glycol (PEG) 20,000 and/or PVP K30 (Vimalson et al., 2018). The authors stated that despite the improved dissolution profile of FENO in the presence of PVP K30, no interaction between drug and excipient was observed by Fourier-transform infrared spectroscopy (FTIR) (Vimalson et al., 2018). Another study on SDs of dipyridamole also employed vibrational spectroscopy and stated that no interaction between dipyridamole and PVP K90 could be detected although there was a stabilizing effect in the SD and a precipitation inhibiting effect of the polymer evidenced (Chauhan et al., 2013). However, it must be noted that FTIR detects peak shifts of excipient-drug mixtures only in the case of strong dipole-mediated interactions, such as hydrogen bonding, leaving hydrophobic molecular interactions practically indetectable. Therefore, assessment of molecular interactions should not be solely based on FTIR, which is currently often the case for interaction assays of solid dispersions that are used in the pharmaceutical industry (Wyttenbach et al., 2013).

Unlike FTIR, nuclear magnetic resonance (NMR) methods provide the means to study hydrophobic interactions, which has been used in recent years to study the effect of polymers to sustain drug supersaturation (Ueda et al., 2013; Ueda et al., 2015; Adhikari and Polli., 2020). Moreover, using different grades of hydroxypropyl methylcellulose acetate succinate, and drugs with varying partition coefficient, the authors of a recent study mentioned the importance of hydrophobic drug interactions regarding precipitation inhibition from supersaturated solutions (Sarabu et al., 2020).

Interesting is a recent work on fluorescence quenching with Stern-Volmer equation analysis to investigate solid dispersions in an aqueous environment. It was reported that depending on the polymer, a fraction of drug appeared to be buried by polymer chains as it was not accessible by the quenching molecule (Aleandri et al., 2018). This is interesting supramolecular information because some polymers were evidently capable of forming hydrophobic pockets (or domains) in which numerous Van der Waals forces can interact with a hydrophobic drug.

This was in line with other recent work of ^{1}H NMR to investigate the interactions of Eudragit EPO with a series of acidic drugs where hydrophobic interactions were reported with polymer side chains as an explanation of the different polymer binding and drug solubilisation observed (Saal et al., 2017). Finally, work on hydroxypropyl cellulose (HPC) to function as a drug precipitation inhibitor suggested that three-dimensional conformations of potentially aggregated polymer chains affected drug solubilisation and precipitation inhibition behavior (Niederquell et al., 2022).

A better understanding of hydrophobic domain formation in common PPIs is of mechanistic interest and it has practical importance especially during the early stages of drug formulation development when different PPIs are screened experimentally for their ability to sustain drug supersaturation. It is hereby a common assumption that at a low concentration of about less than 0.1 % (w/v), a PPI would only act via kinetic effects on maintaining drug supersaturation, whereas a drug solubilising effect can be neglected. However, it is unclear if this is truly the case for a very lipophilic compound like fenofibrate (FENO).

To the best of our knowledge, the present work is the first to combine fluorescence spectroscopy with molecular dynamics (MD) simulations to study hydrophobic domain formation of different PPIs in aqueous solution using FENO as model drug. Fluorescence spectroscopy with pyrene has been used before to characterize the critical micelle concentration of excipients, while in the field of drug supersaturation, the method had previously the aim to identify the onset of a liquid-liquid phase separation from solid dispersions when pyrene can partition into droplets of drug (Ilevbare and Taylor., 2013). However, the current study uses this environment-sensitive molecule differently to probe the supramolecular hydrophobic domain formation of PPIs, which is complemented by full atomistic MD simulations. A final aim was to better understand how hydrophobic domains of typical PPIs would relate to excipient performance regarding kinetic precipitation effects and thermodynamic drug solubilisation at low polymer concentrations.

2. Materials and methods

2.1. Materials

Pyrene, FENO, PVP K30, PVP-VA, and PEG 20,000 were purchased from Sigma Aldrich (Buchs, Switzerland) while Soluplus and Poloxamer 188 were obtained from BASF (Ludwigshafen, Germany). HPMC-603 was obtained from Shin-Etsu Chemical Co. (Tokyo, Japan) and acetonitrile was sourced from Sigma Aldrich (LiChrosolv; gradient grade for liquid chromatography, Supelco, Sigma-Aldrich). Purified water was taken from the MilliQ Millipore filter system (Millipore Co., Bedford, MA, USA). The different chemical structures of the model drug, fluorescent probe, and polymeric excipients are displayed in Fig. 1.

2.2. Fluorescence spectroscopy

The ability of polymers to form hydrophobic pockets was investigated using the environment- sensitive, fluorescent probe, pyrene. The emission spectrum of pyrene was obtained by excitation at 334 nm and measured at room temperature using Agilent Technologies Cary Eclipse fluorescence spectrometer and emission spectra were recorded between 360 and 500 nm with a scanning speed of 240 nm/s. Excitation and emission slit widths were set at 5 nm and 1.5 nm, respectively. The ratio of emission intensities at 374 and 386 nm (I_1/I_3) was measured in different polymer solutions at concentrations between 0.01 and 1 % (w/v), and a pyrene concentration of 40 ng/mL.

2.3. Non-sink supersaturation - solvent shift method

To assess the effectiveness of the polymeric precipitation inhibitors, supersaturation kinetics of FENO were studied in solvent shift experiments. An amount of FENO stock solution in DMSO, necessary to generate a tenfold supersaturation, was added to 50 mL of 0.01 % (w/v) polymer solutions in water. The samples were shaken at 220 rpm and 37 °C in a shaking incubator (Edmund Bühler TH15, Germany) and sampled at different time points. FENO concentrations over time were then measured by high performance liquid chromatography (HPLC) as described in the following section.

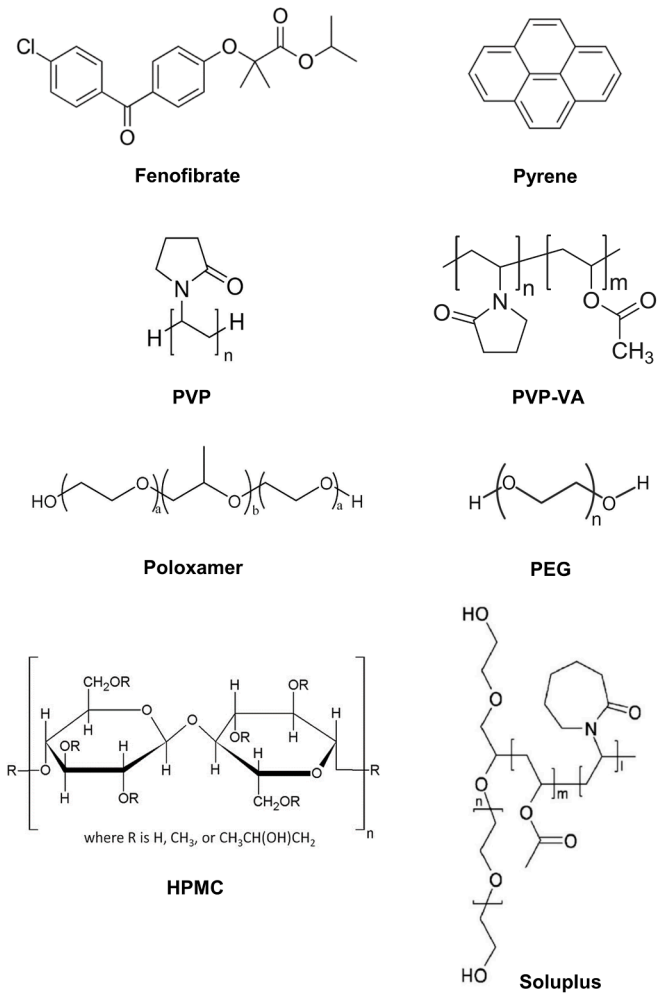

Fig. 1. Chemical structures of the model drug fenofibrate, the fluorescent probe pyrene, and the different polymeric precipitation inhibitors.

2.4. HPLC quantification of FENO from kinetic concentrations

HPLC was used for quantification of FENO in the different supersaturated polymer solutions. Analysis was performed using an Agilent Technologies HPLC, 1200 series and Zorbax Eclipse Plus reverse-phase C18 column (2.1 × 150 mm, 5 µm). The column was maintained at 25 °C. The injection volume was 20 µL and UV absorbance was monitored at 286 nm. Mobile phase was composed of 100 % acetonitrile (A) and water (B), respectively. The flow rate of the instrument was set to 1 mL/min with a run time of 7 min per injection. For 5 min the composition of the mobile phase was set at 70 % solvent A and 30 % solvent B. This was followed by a linear increase of solvent A for 30 s to 90 % acetonitrile and a gradual return to 70 % acetonitrile at 7 min. Finally, apparent supersaturation values were calculated from the ratio of kinetic concentrations divided by the respective equilibrium solubility (where the latter values were obtained as described in the following Section 2.5).

2.5. Miniaturised equilibrium solubility assay

The solubility of FENO was measured in aqueous solutions containing 0, 0.01, 0.05, 0.1, 0.25, 0.5 and 1 % (w/v) polymer. Polymer solutions were prepared by dissolving the adequate amount of excipient in water, stirring for 24 h and diluting appropriately if necessary.

Solubility measurements were conducted according to a slightly modified version of a method previously described by Wyttenbach and co-workers (Wyttenbach et al., 2007). Parylene coated stirring bars (VP 711D, 1.98 mm diameter, 4.80 mm length) and subsequently drug substance were volumetrically dispensed into a 96-well plate (Microplate 96/F-PP; white border; Eppendorf AG) through a manual powder dispenser for 96-well plates. 200 µL of aqueous polymer solutions were pipetted into each well, followed by a 24 h equilibration step by head-over-head rotation (Reax 2; Heidolph) at 37 °C where each well was sealed with pre-split seals (SepraSeal™; Thermo Scientific). After equilibration, drug-polymer suspensions were transferred to a 96-well filter plate (MultiScreen®, Merck Millipore; MSSLBC10; polyvinylidene fluoride) and separated from excess solid by centrifugation into a 96-well plate (twin.tec PCR plate 96; skirted; Eppendorf AG). Filtrates were diluted appropriately with acetonitrile:water mixture (50:50, v/v) using a Gilson positive displacement pipette to enable quantification via Ultra Performance Liquid Chromatography (UPLC). Samples were separated on an Acquity UPLC BEH C18 column (2.1 × 50 mm, 1.7 µm particle size) from Waters™ fitted with a 2996 Photodiode Array Detector. The mobile phase was composed of 0.01 % (v/v) formic acid in water (A) and acetonitrile (B), respectively. The flow rate of the instrument was set to 0.75 mL/min with a run time of 1.2 min per injection. For 0.3 min, the composition of the mobile phase was kept constant by applying an isocratic flow of 40 % solvent A and 60 % solvent B followed by a linear increase of solvent B for 0.5 min up to 100 %. FENO was detected at a wavelength of 286 nm. Residual solid-state analysis by X-ray powder diffraction did not suggest a solvent-mediated phase change. Following these experiments in triplicates, possible outlier samples of HPMC were repeated in a second set of solubility trials for confirmation with again $n = 3$ on a 10 mL scale, while using the same equilibration as stated above.

2.6. Molecular modeling

MD simulations were based on the YASARA software v. 20.12.24 (YASARA Biosciences GmbH, Vienna, Austria) (Krieger and Vriend, 2015). Calculations on central processing units (CPUs) were complemented by determination of Van der Waals and real-space Coulomb forces by use of graphics processing units (GPUs) (Krieger and Vriend, 2015). A general AMBER force field, GAFF2 was employed, wherein atomic charges were based on semi-empirical quantum chemical calculations (AM1BCC) (Jakalian et al., 2002; Wang et al., 2004). All molecules were energy-minimised before they were placed within a simulation box that was then filled with water (TIP3P model) so that the system was of the order of 100 000 – 130 000 atoms (Jorgensen et al., 1983).

To model the different polymeric excipients, simplified chemical structures were selected. Thus, polyvinyl pyrrolidone (PVP K30) was modeled with $n = 80$ monomers by keeping tacticities of adjacent pairs of monomers close to a random distribution in line with the literature (Xiang and Anderson, 2005). The corresponding vinyl acetate co-polymer, PVP-VA, was modeled as a random co-polymer with a total of $n = 80$ units while PEG 20,000 was represented by $n = 75$ units in the polymer. Poloxamer 188 was in the simulations represented by a simpler structure that corresponded to the grade poloxamer 185 and hydroxypropyl methyl cellulose (HPMC), which was modeled with $n = 40$ units with substitution patterns according to the literature (Ueda et al., 2014). Finally, Soluplus, which is a polymeric surfactant having a polyethylene glycol backbone grafted with a copolymerised polyvinyl caprolactam-polyvinyl acetate side chain was modelled with a simplified structure with shorter backbone and side chains of $n = 60$ monomeric units (Mateos et al., 2022). Based on the amphiphilic nature of Soluplus and Poloxamer 188, an aggregation to polymeric micelles was expected and therefore, 20 molecules were placed in the initial simulation box. This opposed to the other polymers for which the simulation box was smaller with only five polymeric excipients but in all cases, every simplified polymeric excipient was matched with a molecule of FENO for modeling purpose.

The simulations made use of periodic boundary conditions.

Following the steepest decent and simulated annealing minimizations to remove clashes, the main simulation was run for 20 ns at 310 K. Equations of motion were integrated with a 2 × 1 fs timestep as an isothermal-isobaric (NTP) ensemble where the pressure control was achieved by rescaling the simulation cell along the x-, y-, and z-axis to reach a constant pressure of 1 bar. A cutoff value of 8 Å was selected for the Van der Waals forces and the particle mesh Ewald algorithm was applied to electrostatic forces (Essmann et al., 1995). Finally, energy calculations were made based on means of ten snapshot calculations during 200 ps following the main simulation runs.

2.7. Statistical data analysis

Statistical data evaluation was based on Statgraphics Centurion 18th Professional edition (v. 18.1.06) from Statgraphics Technologies Inc. (Warrenton, USA). Analysis of variance (ANOVA) used *p*-values for the assumption of the null hypothesis to be true. Low *p*-values of < 0.05 were considered as significant evidence to reject the null hypothesis. Post-hoc comparison between groups was conducted using Tukey's honestly significant difference (HSD) at the 95 % significance level.

3. Results and discussion

3.1. Experimental ability of the polymers to form hydrophobic domains

Six pharmaceutically relevant polymers were selected for investigation of their ability to form hydrophobic microenvironments using fluorescence analysis. The environment-sensitive probe pyrene was used for this purpose. A polarity change in the environment surrounding pyrene results in a shift of its absorption peaks at 374 nm (I_1) and 386 nm (I_3). The ratio of the fluorescence intensities, at these wavelengths, also called the hydrophobic index or I_1/I_3 ratio, was used to study the polymers' ability to form hydrophobic domains (i.e. microenvironments), where hydrophobic drugs, similarly to pyrene, may nest. Fig. 2 shows that all polymers resulted in decreased I_1/I_3 ratio values when compared to a blank reference with just pyrene in water. These changes showed interestingly a clear concentration dependence only in the case of PVP K30, PVP-VA and Soluplus.

The most pronounced decrease in I_1/I_3 ratio was observed for PVP K30 together with Soluplus, although only the latter is an amphiphilic micelle-forming polymer. However, this was explained by the known high flexibility of PVPs, whose structure can easily transition from a coil to a more globule-like structure depending on the balance of attractive and repulsive forces between polymer chains (Voronova et al., 2018). Given high polymer flexibility, multiple small loops can be formed to offer a microenvironment where hydrophobic compounds can be embedded. The obtained decreases in I_1/I_3 values in case of PVP indicated that such hydrophobic domain formation was even comparable to that of a micelle-forming excipient such as Soluplus.

While pyrene was expected to partition into the hydrophobic core of polymeric micelles formed by Soluplus, it was an interesting finding that I_1/I_3 decreased less for Poloxamer 188, although the latter excipient has an amphiphilic structure too and can form polymeric micelles as well. However, Soluplus is significantly more lipophilic than Poloxamer 188 because the former is composed of vinylcaprolactam and vinylacetate, whereas the latter has a higher percentage of the hydrophilic polyethylene oxide blocks (Russo and Villa, 2019; Voronova et al., 2018). The degree of lipophilic components in the polymer would then define the hydrophobicity of microenvironments forming upon aqueous dispersion. Thus, the observed I_1/I_3 decreases of pyrene solutions with excipient as compared to the blank pyrene reference were not only determined by the extent of PPI domain formation but also by their polarity as both factors drive partitioning of pyrene.

Furthermore, the critical micellar concentration, CMC, of Soluplus was reported to be clearly lower than that of Poloxamer 188 (0.5 mg/mL versus 4.1 mg/mL, at 37 °C) (Alopaeus et al., 2019). It should be noted that hydrophobic pocket formation was studied at room temperature but since CMC typically decreases monotonically with increasing temperature (Kroll et al., 2022), the CMC of both polymers was expected to slightly increase at 25 °C but would still result in a relatively lower CMC value for Soluplus compared to Poloxamer. Therefore, given the relatively higher lipophilicity and lower CMC of Soluplus, it is

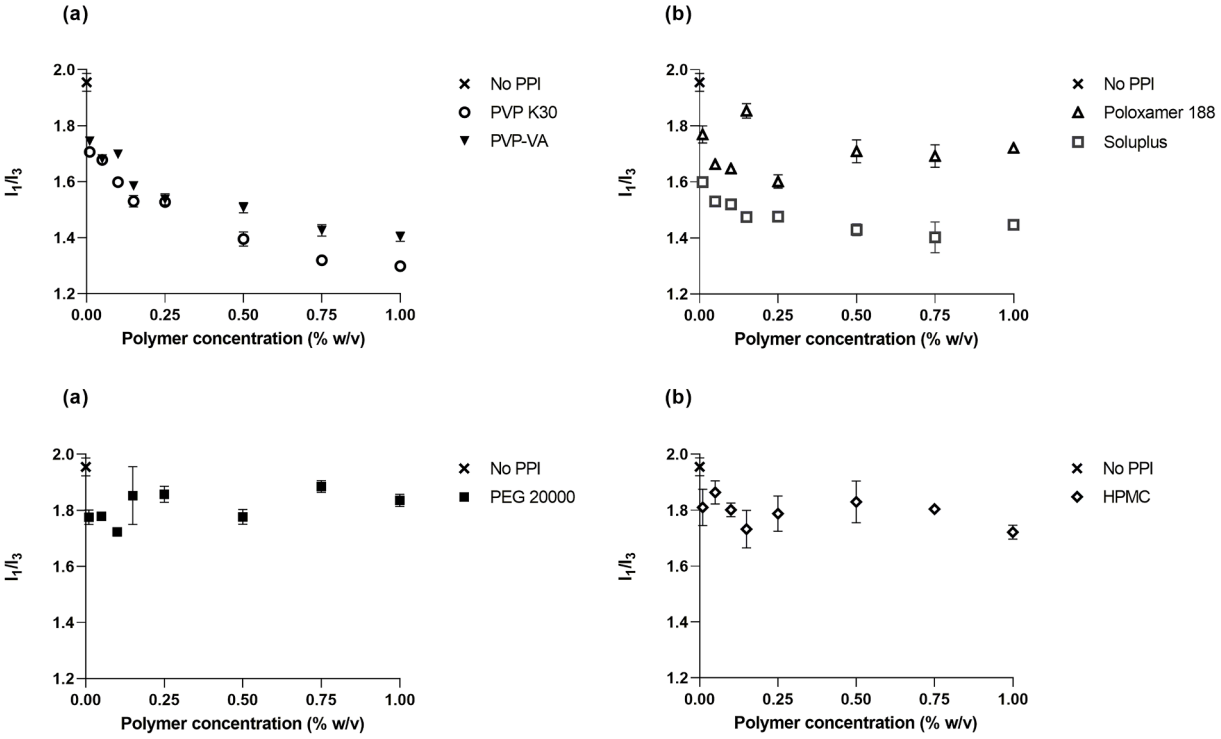

Fig. 2. Hydrophobic index (I_1/I_3) for pyrene luminescence for different types and concentrations of polymers tested (panel (a)-(d), $n = 3$).

understandable that this PPI resulted in more pronounced decreases of I_1/I_3 as compared to those of Poloxamer.

The I_1/I_3 data from the investigations of HPMC did not suggest a great tendency to form hydrophobic domains. The polymer is known to aggregate at temperatures higher than 55 °C (depending on the used grade) and would likely require higher concentrations than used in the present study to form hydrophobic regions (Silva et al., 2008). Comparatively low decreases of I_1/I_3 were also evidenced for PEG 20,000, which was in line with the high hydrophilicity of the polymer. This hydrophilicity can be quantified in terms of relative permittivity and the latter value for PEG was previously found to be higher than that of diverse less polar pharmaceutical excipients, but it was still clearly lower than the relative permittivity of water (Niederquell et al., 2019). Therefore, PEG is only comparatively hydrophilic but PEG microdomains can still form on dispersion based on the polarity difference to water, which was supported by the experimentally observed slight decreases of I_1/I_3 values relative to pure water (Fig. 2).

3.2. Molecular simulations and formation of hydrophobic microenvironments

Computer simulations have become an effective visualization tool and are of great help in rationalizing experimental data (Gupta et al., 2005). In the present study MDs were used, in conjunction to the hydrophobic index scale, to elucidate the interactions theoretically taking place between FENO and the different polymers in solution.

Fig. 3 shows that excipient aggregation and a kind of polymeric-micelle formation was obtained in the MD simulations with Soluplus and Poloxamer 188. Thus, both types of polymers displayed extensive formation of hydrophobic domains in agreement with the experimental data described above.

As for the relatively greater extent of I_1/I_3 decrease for Soluplus compared to Poloxamer 188, the atomistic model did not support a mechanism solely based on geometric aspects of the polymeric micelle. There was no marked difference in surface versus core solubilisation of FENO with respect to micelle packing density, rather did the MD simulations suggest that Poloxamer 188 appeared to form a denser aggregate. This supports the discussion of I_1/I_3 decreases in the previous Section 3.1. where this difference between these two micelle-forming polymers was attributed to the chemical nature of the microenvironments as Soluplus offered a lower polarity compared to Poloxamer 188. Another aspect of the specific polymer chemistry was that only with Soluplus, occasional hydrogen bonding, was observed where some of the FENO molecules were hydrogen bond accepting. This contributed on the average to about 5 % of the total interaction energy, hence Van der Waals interactions were still dominating the PPI interaction with FENO. Fig. 4 displays MD snapshots for the other tested polymers where no polymeric micelle formation was expected at given experimental conditions, i.e., HPMC, PVP K30, and PVP-VA.

High chain flexibility of PVP K30 and PVP-VA was observed in the MD simulations in that tightly packed chain loops were surrounding FENO, which was embedding the drug similar to an inclusion in a polymeric micelle. This was in good agreement with the pronounced decreases of I_1/I_3 values that were observed for these highly flexible polymers. However, the geometric part of the pocket formation was one aspect, while the chemical nature of the polymer was another. The pyrrolidone-based polymers offered a less polar microenvironment than polyethylene glycol, which explained the moderate experimental I_1/I_3 decreases observed with PEG 20,000 although the MD simulation demonstrated also a high polymeric flexibility and coil formation in line with the literature (Alessi et al., 2005). Noteworthy for the PEG 20,000 was that FENO molecules appeared to be less separated than in the case of the other polymers in their respective MD simulations. Thus, pi-pi interactions were observed between individual FENO molecules. These self-interactions of the very hydrophobic model drug indicate that PEG 20,000 did not offer polymeric domains of sufficient solvation capacity to fully overcome drug self-cohesion.

While there was domain formation and integration of FENO observed for PEG 20,000, the MD results for HPMC provided a different picture (Fig. 4). Owing to the β−1,4-glycosidic bonds of the monomers, cellulose-based polymers are comparatively rigid. This was reflected in the MD simulations by the absence of small chain loops for drug nesting, which was otherwise observed with the other more flexible polymers. A rigid polymer such as HPMC would require entire chains to aggregate to form hydrophobic domains but individual hydrophobic interactions can still occur. Thus, a recent study of FENO and a cellulosic polymer was making use of different NMR techniques to show that hydrophobic interactions occurred via the pyranose ring and the diphenyl ketone of FENO as well as via side chains such as with methyl groups (Martin-Pastor and Stoyanov, 2021). The present MD simulations in case of HPMC supported this view that hydrophobic interactions occurred but not via embedding of drug in entire domains but rather along a single chain of the polymer. This result was also in agreement with the comparatively low I_1/I_3 decreases of HPMC (Fig. 2). Interestingly, the simulations revealed further that some hydrogen bonding occurred between FENO and HPMC, where FENO was an acceptor, and the associated energy was about 19 % of the overall interaction energy with HPMC.

3.3. Effect of polymers on kinetic concentrations and apparent supersaturation

To evaluate the relationship between the tendency of a polymer to form hydrophobic domains and its ability to maintain high kinetic drug concentrations, a non-sink *in vitro* test was performed. Fig. 5 shows kinetic concentration curves of FENO in the different polymer solutions.

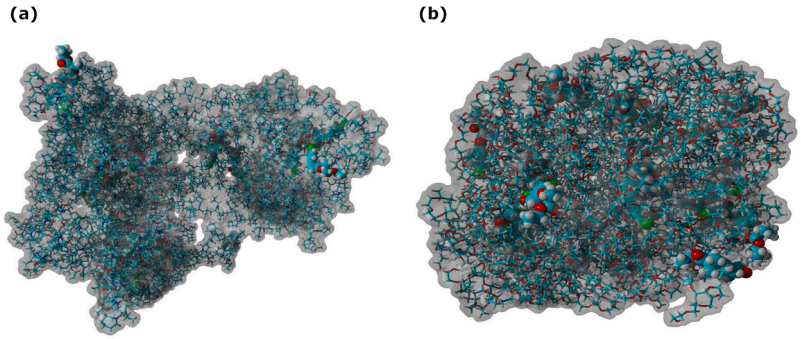

Fig. 3. Snapshot of a molecular dynamics (MD) simulation (20 ns), which shows fenofibrate and excipients that are polymeric micelle formers, i.e., (a) Soluplus and (b) Poloxamer 188, in water (TIP3P model). The polymeric Van der Waals surface is depicted, and drug molecules are given as space-filled model, while water molecules are not shown for clarity of presentation.

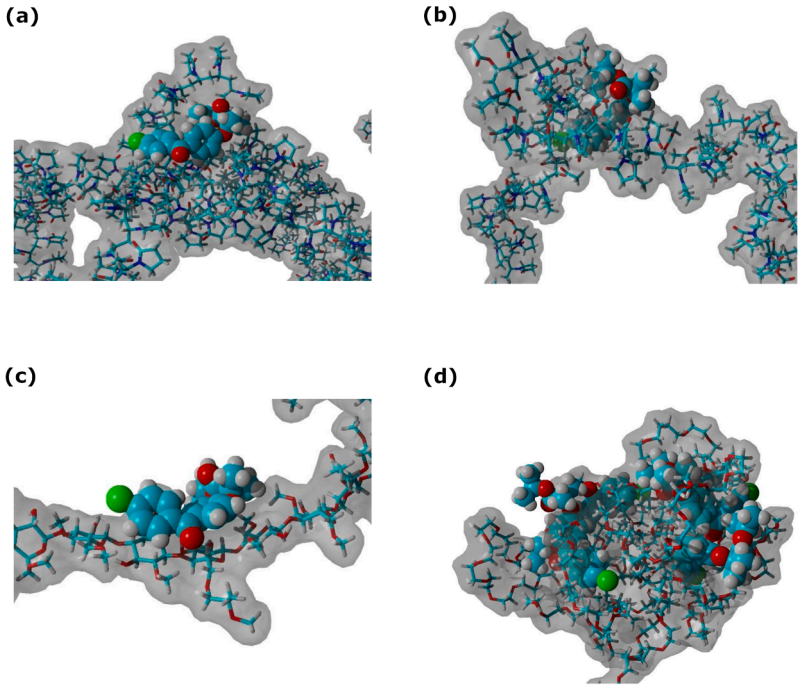

Fig. 4. Magnified view of a snapshot MD simulation (20 ns) of fenofibrate and polymers, (a) PVP K30, (b) PVP-VA, (c) HPMC, (d) PEG 20,000, in water (TIP3P model). The polymeric Van der Waals surface is depicted, and drug molecules are given as space-filled model, while water molecules are not shown for clarity of presentation.

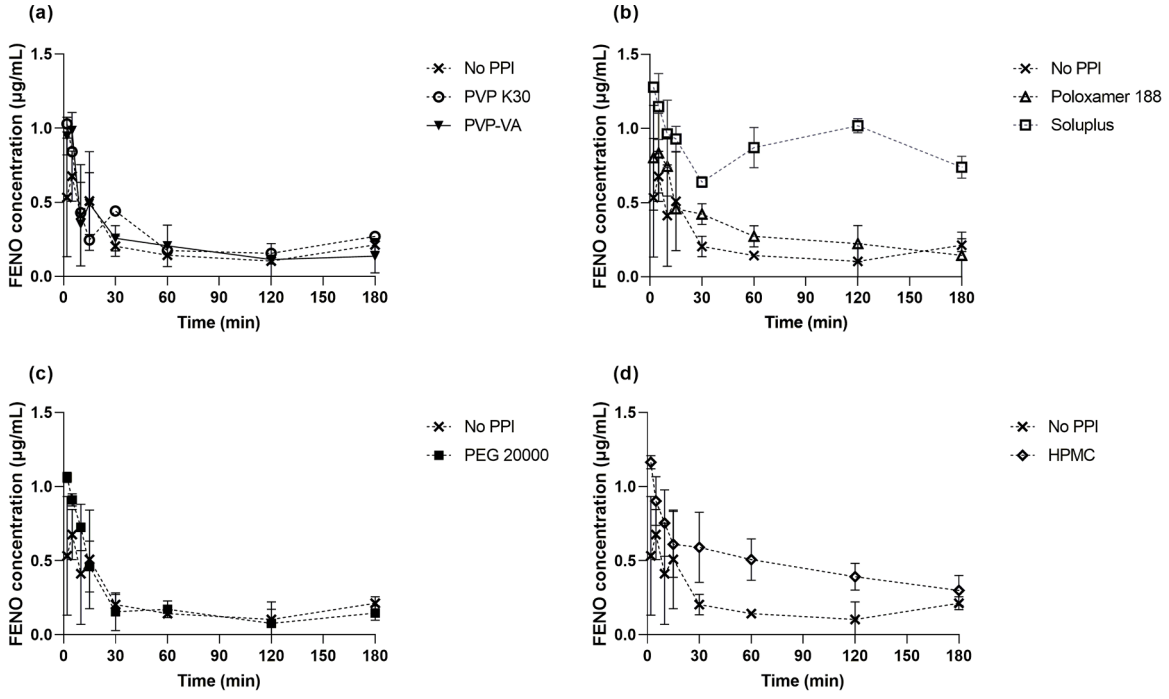

Fig. 5. Kinetic concentrations of fenofibrate (µg/mL) vs. time (min) at 37 °C in 0.01 % (w/v) polymer in aqueous solution (panel (a)-(d), $n = 3$).

As a result, higher concentrations were generally observed in solutions with PPI as compared to FENO solutions without added PPI. However, not all excipients showed clear differences especially during later timepoints in the experiment.

Considering the concentrations over time (Fig. 5), Soluplus was the best-performing polymer at maintaining high kinetic concentrations for the full duration of the experiment. Comparatively high concentrations were also sustained in presence of HPMC (Fig. 5). The latter polymer has been shown earlier to exhibit kinetic effects on the surface of nuclei and growing crystals (Chauhan et al., 2013; Gao et al., 2009; Warren et al., 2010). Ziller et al. proposed that HPMC acts as a mechanical barrier to crystallization by preventing drug molecules in solution from adsorbing to the crystal lattice (Gao et al., 2009; Ziller and Rupprecht, 1988). However, it is important to differentiate kinetic effects from pure solvation effects and therefore, solubility values at 0.01 % (w/v) of PPI were used to normalise the concentrations to obtain apparent

supersaturation values over time (Fig. 6).

There were notable solubilisation effects observed that caused reduced apparent supersaturation compared to the blank solution without PPI. The apparent supersaturation was most dominantly reduced in case of the aforementioned HPMC but also with PVP K30, PVP-VA, Soluplus, and Poloxamer, the decreases in supersaturation reduced the driving force of drug precipitation.

Regarding the latter micelle-forming excipients, Soluplus showed higher concentrations relative to Poloxamer 188 (Fig. 5) and given the reduced apparent supersaturation of both polymers (Fig. 6), concentration-time profiles were apparently influenced by kinetic effects, whereby the less hydrophobic chemical nature of Poloxamer compared to Soluplus was likely causing the difference in sustaining drug concentrations over time (Alopaeus et al., 2019; Russo and Villa, 2019).

Moreover, PVP K30 and PVP-VA were also not showing high and sustained FENO concentrations over time (Fig. 5). Some precipitation apparently occurred over time although the supersaturation kinetics revealed that the driving force of such precipitation was clearly reduced compared to the blank reference without PPI (Fig. 6). Interestingly, a previous study on monomer contributions to precipitation inhibition performance concluded that the more hydrophobic monomer vinyl acetate was more relevant than vinylpyrrolidone for stabilization of supersaturated celecoxib (Knopp et al., 2016). However, the present study did not show a marked difference between PVP K30 and PVP-VA in their kinetic concentration profiles in case of FENO.

Finally, PEG 20,000 showed a rapid drop in kinetic concentrations similar to the reference without PPI (Fig. 5). One aspect of this observation was the obviously limited capacity of PEG 20,000 to prevent drug precipitation while another is that apparent supersaturation was clearly higher than with the other PPIs (Fig. 6), which was mainly due to a lacking solubilisation capacity of this PPI at the 0.01 % (w/v) level.

An overview of maximum supersaturation is given by Table 1 together with 95 % confidence intervals of the ANOVA. The latter Tukey's HSD intervals were comparatively broad, which is not unusual for non-sink supersaturation experiments because drug precipitation is a stochastic process that comes with a high inherent variability. The ANOVA still shows differences between the samples ($p < 0.0001$) in terms of maximum supersaturation in that the reference without PPI and PEG 20,000 were significantly different from the group of other polymers. The latter group of polymers showed some tendencies regarding maximum supersaturation values, but these more subtle differences were better seen in the overall time course of the non-sink *in vitro* test as it was discussed above.

Table 1
Maximum supersaturation and ANOVA 95 % Tukey's HSD intervals.

	Maximum supersaturation as means ($n = 3$)	Maximum supersaturation as 95 % Tukey confidence intervals
No PPI	12.2	10.0 - 14.4
PVP K30	1.9	−0.3 - 4.2
PVP-VA	1.3	−0.9 – 3.6
PEG 20,000	9.0	6.8 - 11.3
HPMC	1.4	−0.9 – 3.6
Poloxamer 188	1.7	−0.6 - 3.9
Soluplus	3.1	0.8 - 5.3

3.4. Impact of different polymer concentrations on drug solubility

To explore the drug solubilising effects of the PPIs not only at the diluted 0.01 %, w/v level, further higher concentrations were analysed in line with ranges used for the fluorescence study. The results of the thermodynamic solubility values of FENO are show in Fig. 7.

Solubilising effects of polymer on drugs are complex and dependent on many parameters, such as type of drug, type of polymer and polymer concentration. A nearly linear solubilising effect of FENO with increasing polymer concentration was observed with Soluplus (Fig. 7). This was attributed to the amphiphilic excipient nature where the dissolved drug is incorporated within the lipophilic core of polymeric micelles in line with the results of the present work as well as previous research (Alopaeus et al., 2019).

Poloxamer 188, PVP K30, PVP-VA and PEG 20,000 did not exhibit a pronounced concentration effect, which was analogous to what has been reported before, for example in the case of rivaroxaban (Choi et al., 2022; Lee et al., 2021). Finally, HPMC displayed a more complex concentration effect on FENO solubilisation. Albeit, significantly improving overall drug solubility, an increase in polymer concentration resulted in

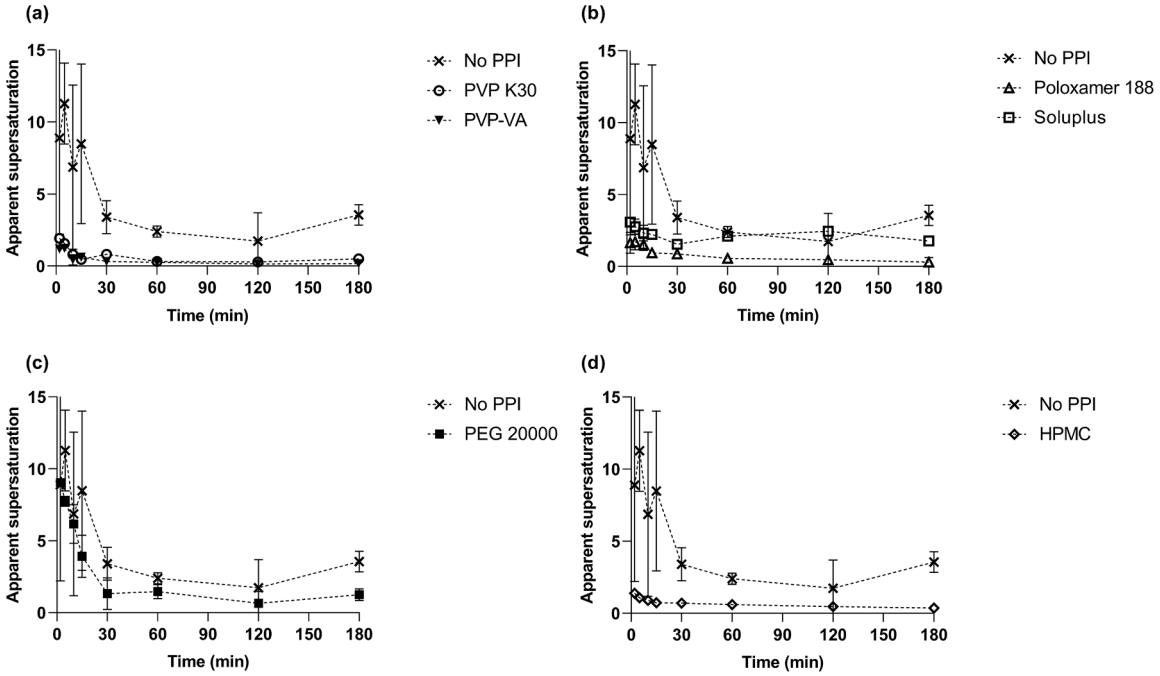

Fig. 6. Apparent supersaturation of fenofibrate vs. time (min) at 37 °C in 0.01 % (w/v) polymer in aqueous solution (panel (a)-(d), $n = 3$).

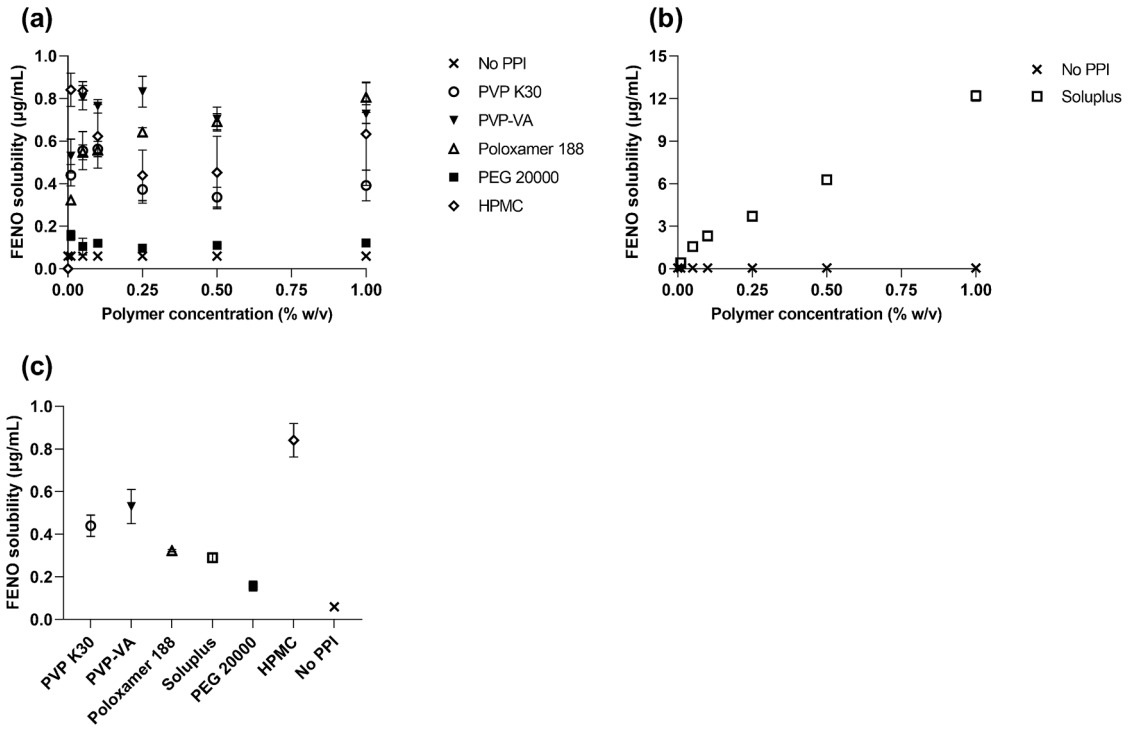

Fig. 7. (a) and (b) Solubility of fenofibrate (µg/mL) for different polymers and polymer concentrations and (c) solubility at 0.01 % (w/v) polymer in aqueous solution ($n = 3$).

a reduced solubilising benefit within the concentration range studied. The study with rivaroxaban also observed an analogues relationship where increasing concentrations of HPMC led to a reduced drug solubilisation (Choi et al., 2022; Lee et al., 2021). As the present study indicated a direct molecular interaction of free HPMC chains with FENO, the accessibility of such free polymer chains is apparently in competition with the known self-interaction of the chains, which is depending on HPMC concentration and temperature (Joshi, 2011). Therefore, it is understandable that HPMC showed diminishing solubilisation gains of FENO with increasing polymer concentration at least for up to 1 % (w/v).

The diluted situation with very low polymer concentration (0.01 %, w/v) provided FENO solubility values that were clearly higher than the reference without PPI but still below a concentration order of 1 µg/mL (Fig. 7). It should be noted that a solubility ranking between polymers was depending on polymer concentration, which reflected the previously discussed complex concentration-dependence of drug solubilisation. Accordingly, specific polymer characteristics must be considered. Despite of the low polymer level of 0.01 % (w/v), solubilising effects were observed for PVP K30 and PVP-VA in accordance with the discussed hydrophobic domain formation of these highly flexible polymers. Such hydrophobic domains as indicated by the pyrene-fluorescence data and MD simulations, were also the expected reason for the observed FENO solubilisation of Soluplus. However, the extent of solubilisation was clearly below that of higher Soluplus levels for which a more pronounced micelle formation was assumed that would cause a nearly linear increase (Fig. 7).

In the case of Poloxamer 188, previous studies have shown that the extent of drug incorporation in poloxamers strongly depended on the hydrophobic/hydrophilic ratio of the polymer and the drug loading capacity was related to the CMC and critical micelle temperature (CMT) (Olea et al., 2014; Santander-Ortega et al., 2006). Given the previously mentioned CMC of Poloxamer 188 at 37 °C, it was not expected that a pronounced micelle formation was causing the rather moderate drug solubilisation at 0.01 % w/v (Fig. 7).

The high solubilisation of FENO by the low concentration of HPMC was most remarkable. It was in line with the non-sink *in vitro* results in that the thermodynamic driving force for precipitation was apparently reduced by the solubilising effect of HPMC. The data of fluorescence analysis together with the MD simulations suggested that this effect was the result of direct drug and polymer-chain interactions, whereas there was no support for the alternative view of a supramolecular domain formation at this low HPMC concentration. As mentioned in the discussion of the in silico results, the interaction of FENO and HPMC involved also hydrogen bonding, which was further promoting the observed drug solubilisation.

It was overall remarkable that all PPIs displayed notable solubilising effects of FENO even at the very low polymer concentration of 0.01 % w/v. Although it is often assumed for such low polymer concentrations that primarily kinetic effects on the surface of nuclei/crystals or in solution phase cause the performance of PPIs, the present study demonstrated clear solubilising effects in case of the very lipophilic model compound FENO.

4. Conclusion

In this study, the ability of pharmaceutical polymers to form hydrophobic domains was investigated by means of fluorescence spectroscopy as well as atomistic MD simulations. These results were compared to the polymer performance in terms of their ability to maintain supersaturation and to facilitate solubilisation of the model drug FENO. Notable was the observation how highly flexible polymers form multiple loops that can embed a drug in hydrophobic environments. This was quite different for the more rigid polymer HPMC, but strong drug-polymer interactions were also found here because the multiple Van der Waals interactions with individual HPMC chains were complemented with some hydrogen bonding. Finally, HPMC and Soluplus could both sustain high kinetic drug concentrations in the solvent-shift experiments whereby an increased solubility and reduced supersaturation was of relevance.

An understanding of hydrophobic domain formation in aqueous dispersion is important but it should be considered that the performance

of a PPI is the result of both thermodynamic solubility as well as kinetic effects. Therefore, further research is needed with additional compounds and polymers to obtain a broader view on individual factor contributions to excipient performance. However, it can be already concluded that the approach of fluorescence analysis in conjunction with full atomistic MD simulations provided valuable insights into the molecular architecture of the individual PPIs and in how they interact with a lipophilic drug.

CRediT authorship contribution statement

Egis Zeneli: Writing – original draft, Investigation, Formal analysis. **Justus Johann Lange:** Writing – review & editing, Investigation. **René Holm:** Writing – review & editing, Supervision. **Martin Kuentz:** Writing – review & editing, Supervision.

Data availability

Data will be made available on request.

Acknowledgments

This project has received funding from the European Union's Horizon 2020 research and innovation program under the Marie Skłodowska-Curie grant agreement No 955756.

References

Adhikari, A., Polly, J.E., 2020. Characterization of grades of HPMCAS spray dried dispersions of itraconazole based on supersaturation kinetics and molecular interactions impacting formulation performance. Pharm. Res. 37, 192.

Aleandri, S., Jankovic, S., Kuentz, M., 2018. Towards a better understanding of solid dispersions in aqueous environment by a fluorescence quenching approach. Int. J. Pharm. 550, 130–139. https://doi.org/10.1016/j.ijpharm.2018.08.029.

Alessi, M.L., Norman, A.I., Knowlton, S.E., Ho, D.L., Greer, S.C., 2005. Helical and coil conformations of poly(ethylene glycol) in isobutyric acid and water. Macromolecules 38, 9333–9340. https://doi.org/10.1021/ma051339e.

Alopaeus, J.F., Hagesæther, E., Tho, I., 2019. Micellisation mechanism and behaviour of Soluplus®–furosemide micelles: preformulation studies of an oral nanocarrier-based system. Pharmaceuticals 12. https://doi.org/10.3390/ph12010015.

Boyd, B.J., Bergström, C.A.S., Vinarov, Z., Kuentz, M., Brouwers, J., Augustijns, P., Brandl, M., Bernkop-Schnürch, A., Shrestha, N., Préat, V., Müllertz, A., Bauer-Brandl, A., Jannin, V., 2019. Successful oral delivery of poorly water-soluble drugs both depends on the intraluminal behavior of drugs and of appropriate advanced drug delivery systems. Eur. J. Pharm. Sci. 137 https://doi.org/10.1016/j.ejps.2019.104967.

Chauhan, H., Hui-Gu, C., Atef, E., 2013. Correlating the behavior of polymers in solution as precipitation inhibitor to its amorphous stabilization ability in solid dispersions. J. Pharm. Sci. 102, 1924–1935. https://doi.org/10.1002/jps.23539.

Chavan, R.B., Thipparaboina, R., Kumar, D., Shastri, N.R., 2016. Evaluation of the inhibitory potential of HPMC, PVP and HPC polymers on nucleation and crystal growth. RSC Adv. 6, 77569–77576. https://doi.org/10.1039/c6ra19746a.

Choi, M.J., Woo, M.R., Choi, H.G., Jin, S.G., 2022. Effects of polymers on the drug solubility and dissolution enhancement of poorly water-soluble Rivaroxaban. Int. J. Mol. Sci. 23 https://doi.org/10.3390/ijms23169491.

Ditzinger, F., Price, D.J., Ilie, A.R., Köhl, N.J., Jankovic, S., Tsakiridou, G., Aleandri, S., Kalantzi, L., Holm, R., Nair, A., Saal, C., Griffin, B., Kuentz, M., 2019. Lipophilicity and hydrophobicity considerations in bio-enabling oral formulations approaches – a PEARRL review. J. Pharm. Pharmacol. https://doi.org/10.1111/jphp.12984.

Ducker, W.A., Mastropietro, D., 2016. Forces between extended hydrophobic solids: is there a long-range hydrophobic force? Curr. Opin. Colloid Interface Sci. https://doi.org/10.1016/j.cocis.2016.02.006.

Essmann, U., Perera, L., Berkowitz, M.L., Darden, T., Lee, H., Pedersen, L.G., 1995. A smooth particle mesh Ewald method. J. Chem. Phys. 103, 8577–8593. https://doi.org/10.1063/1.470117.

Feng, D., Peng, T., Huang, Z., Singh, V., Shi, Y., Wen, T., Lu, M., Quan, G., Pan, X., Wu, C., 2018. Polymer–surfactant system based amorphous solid dispersion: precipitation inhibition and bioavailability enhancement of itraconazole. Pharmaceutics 10. https://doi.org/10.3390/pharmaceutics10020053.

Gao, P., Akrami, A., Alvarez, F., Hu, J., Li, L., Ma, C., Surapaneni, S., 2009. Characterization and optimization of AMG 517 supersaturatable self-emulsifying drug delivery system (S-SEDDS) for improved oral absorption. J. Pharm. Sci. 98, 516–528. https://doi.org/10.1002/jps.21451.

Gupta, P., Thilagavathi, R., Chakraborti, A.K., Bansal, A.K., 2005. Role of molecular interaction in stability of celecoxib-PVP amorphous systems. Mol. Pharm. 2, 384–391. https://doi.org/10.1021/mp050004g.

Ilevbare, G.A., Taylor, L.S., 2013. Liquid–liquid phase separation in highly supersaturated aqueous solutions of poorly water-soluble drugs: implications for solubility enhancing formulations. Cryst. Growth Des. 13, 1497–1509.

Jakalian, A., Jack, D.B., Bayly, C.I., 2002. Fast, efficient generation of high-quality atomic charges. AM1-BCC model: II. Parameterization and validation. J. Comput. Chem. 23, 1623–1641. https://doi.org/10.1002/jcc.10128.

Jorgensen, W.L., Chandrasekhar, J., Madura, J.D., Impey, R.W., Klein, M.L., 1983. Comparison of simple potential functions for simulating liquid water. J. Chem. Phys. 79, 926–935. https://doi.org/10.1063/1.445869.

Joshi, S.C., 2011. Sol-gel behavior of hydroxypropyl methylcellulose (HPMC) in ionic media including drug release. Materials 4, 1861–1905 (Basel).

Knopp, M.M., Nguyen, J.H., Mu, H., Langguth, P., Rades, T., Holm, R., 2016. Influence of copolymer composition on *in vitro* and *in vivo* performance of Celecoxib-PVP/VA amorphous solid dispersions. AAPS J. 18, 416–423. https://doi.org/10.1208/s12248-016-9865-6.

Krieger, E., Vriend, G., 2015. New ways to boost molecular dynamics simulations. J. Comput. Chem. 36, 996–1007. https://doi.org/10.1002/jcc.23899.

Kroll, P., Benke, J., Enders, S., Brandenbusch, C., Sadowski, G., 2022. Influence of temperature and concentration on the self-assembly of nonionic C(i)E(j) surfactants: a light scattering study. ACS Omega 7, 7057–7065.

Lee, J.H., Sik Jeong, H., Jeong, J.W., Koo, T.S., Kim, D.K., Cho, Y.H., Lee, G.W., Lee, C.:., Jeong, J.H., Jeong, H.S.;., Koo, J.W., Kim, T.S., Cho, D.K., Lee, Y.H.;., The, G.W., Kachrimanis, K., Bilgili, E., 2021. Pharmaceutics The development and optimization of hot-melt extruded amorphous solid dispersions containing Rivaroxaban in combination with polymers. Pharmaceutics 13, 344. https://doi.org/10.3390/pharmaceutics.

Martin-Pastor, Stoyanov, E., 2021. New insights into the use of hydroxypropyl cellulose for drug solubility enhancement: an analytical study of sub-molecular interactions with fenofibrate in solid state and aqueous solutions. J. Polym. Sci. 59, 1855–1865.

Mateos, H., Gentile, L., Murgia, S., Colafemmina, G., Collu, M., Smets, J., Palazzo, G., 2022. Understanding the self-assembly of the polymeric drug solubilizer Soluplus®. J. Colloid Interface Sci. 611, 224–234. https://doi.org/10.1016/j.jcis.2021.12.016.

Meyer, E.E., Rosenberg, K.J., Israelachvili, J., 2006. Recent progress in understanding hydrophobic interactions.

Niederquell, A., Dujovny, G., Probst, S.E., Kuentz, M., 2019. A relative permittivity approach for fast drug solubility screening of solvents and excipients in lipid-based delivery. J. Pharm. Sci. 108, 3457–3460. https://doi.org/10.1016/j.xphs.2019.06.014.

Niederquell, A., Stoyanov, E., Kuentz, M., 2022. Hydroxypropyl cellulose for drug Precipitation inhibition: from the potential of molecular interactions to performance considering microrheology. Mol. Pharm. 19, 690–703. https://doi.org/10.1021/acs.molpharmaceut.1c00832.

Olea, A.F., Carrasco, H., Espinoza, L., Acevedo, B., 2014. Solubilization of p-alkylphenols in Pluronics F-68 and F-127 micelles: partition coefficients and effect of solute on the aggregate structure. J. Chilean Chem. Soc. 59, 2451–2454. https://doi.org/10.4067/S0717-97072014000200011.

Price, D.J., Ditzinger, F., Koehl, N.J., Jankovic, S., Tsakiridou, G., Nair, A., Holm, R., Kuentz, M., Dressman, J.B., Saal, C., 2019. Approaches to increase mechanistic understanding and aid in the selection of precipitation inhibitors for supersaturating formulations – a PEARRL review. J. Pharm. Pharmacol. https://doi.org/10.1111/jphp.12927.

Russo, E., Villa, C., 2019. Poloxamer hydrogels for biomedical applications. Pharmaceutics. https://doi.org/10.3390/pharmaceutics11120671.

Saal, W., Ross, A., Wyttenbach, N., Alsenz, J., Kuentz, M., 2017. A systematic study of molecular interactions of anionic drugs with a dimethylaminoethyl methacrylate copolymer regarding solubility enhancement. Mol. Pharm. 14, 1243–1250. https://doi.org/10.1021/acs.molpharmaceut.6b01116.

Santander-Ortega, M.J., Jódar-Reyes, A.B., Csaba, N., Bastos-González, D., Ortega-Vinuesa, J.L., 2006. Colloidal stability of Pluronic F68-coated PLGA nanoparticles: a variety of stabilisation mechanisms. J. Colloid Interface Sci. 302, 522–529. https://doi.org/10.1016/j.jcis.2006.07.031.

Sarabu, S., Kallakunta, V.R., Bandari, S., Batra, A., BI, V., Durig, T., Zhang, F., Repka, M.A., 2020. Hypromellose acetate succinate based amorphous solid dispersions via hot melt extrusion: effect of drug physicochemical properties. Carbohydr. Polym. 233, 115828.

Sharma, A., Jain, C.P., 2010. Preparation and characterization of solid dispersions of carvedilol with PVP K30. Res. Pharm. Sci.

Silva, S.M.C., Pinto, F.v., Antunes, F.E., Miguel, M.G., Sousa, J.J.S., Pais, A.A.C.C., 2008. Aggregation and gelation in hydroxypropylmethyl cellulose aqueous solutions. J. Colloid Interface Sci. 327, 333–340. https://doi.org/10.1016/j.jcis.2008.08.056.

Taylor, L.S., Zhang, G.G.Z., 2016. Physical chemistry of supersaturated solutions and implications for oral absorption. Adv. Drug Deliv. Rev. https://doi.org/10.1016/j.addr.2016.03.006.

Tres, F., Hall, S.D., Mohutsky, M.A., Taylor, L.S., 2018. Monitoring the phase behavior of supersaturated solutions of poorly water-soluble drugs using fluorescence techniques. J. Pharm. Sci. 107, 94–102. https://doi.org/10.1016/j.xphs.2017.10.002.

Ueda, K., Higashi, K., Yamamato, K., Moribe, K., 2013. Inhibitory effect of hydroxypropyl methylcellulose acetate succinate on drug recrystallization from a supersaturated solution assessed using nuclear magnetic resonance measurements. Mol. Pharm. 10, 3801–3811.

Ueda, K., Higashi, K., Yamamoto, K., Moribe, K., 2014. The effect of HPMCAS functional groups on drug crystallization from the supersaturated state and dissolution improvement. Int. J. Pharm. 464, 205–213. https://doi.org/10.1016/j.ijpharm.2014.01.005.

Ueda, K., Higashi, K., Yamamato, K., Moribe, K., 2015. Equilibrium state at supersaturated drug concentration achieved by hydroxypropyl methylcellulose acetate succinate: molecular characterization using (1)H NMR technique. Mol. Pharm. 12, 1096–1104.

Vimalson, D.C., Parimalakrishnan, S., Jeganathan, N.S., Anbazhagan, S., 2018. Enhancement of solubility and dissolution characteristics of fenofibrate by solid dispersion technique. Int. Res. J. Pharm. 9, 145–150. https://doi.org/10.7897/2230-8407.0910242.

Voronova, M., Rubleva, N., Kochkina, N., Afineevskii, A., Zakharov, A., Surov, O., 2018. Preparation and characterization of polyvinylpyrrolidone/cellulose nanocrystals composites. Nanomaterials 8. https://doi.org/10.3390/nano8121011.

Wang, J., Wolf, R.M., Caldwell, J.W., Kollman, P.A., Case, D.A., 2004. Development and testing of a general Amber force field. J. Comput. Chem. 25, 1157–1174. https://doi.org/10.1002/jcc.20035.

Warren, D.B., Benameur, H., Porter, C.J.H., Pouton, C.W., 2010. Using polymeric precipitation inhibitors to improve the absorption of poorly water-soluble drugs: a mechanistic basis for utility. J. Drug Target. https://doi.org/10.3109/1061186X.2010.525652.

Wyttenbach, N., Alsenz, J., Grassmann, O., 2007. Miniaturized assay for solubility and residual solid screening (SORESOS) in early drug development. Pharm. Res. 24, 888–898. https://doi.org/10.1007/s11095-006-9205-0.

Wyttenbach, N., Janas, C., Siam, M., Lauer, M., Jacob, L., Scheubel, E., Page, S., 2013. Miniaturized screening of polymers for amorphous drug stabilization (SPADS): rapid assessment of solid dispersion systems. Eur. J. Pharm. Biopharm. 84, 583–598.

Xiang, T.X., Anderson, B.D., 2005. Distribution and effect of water content on molecular mobility in poly(vinylpyrrolidone) glasses: a molecular dynamics simulation. Pharm. Res. 22, 1205–1214. https://doi.org/10.1007/s11095-005-5277-5.

Zhao, P., Han, W., Shu, Y., Li, M., Sun, Y., Sui, X., Liu, B., Tian, B., Liu, Y., Fu, Q., 2023. Liquid-liquid phase separation drug aggregate: merit for oral delivery of amorphous solid dispersions. J. Control Release 353, 42–50.

Ziller, K.H., Rupprecht, H., 1988. Control of crystal growth in drug suspensions: (1) Design of a control unit and application to Acetaminophen suspensions. Drug Dev. Ind. Pharm. 14, 2341.